



UNIVERSITY OF LEEDS

This is a repository copy of *Stability of a Class of Delayed Port-Hamiltonian Systems with Application to Droop-Controlled Microgrids*.

White Rose Research Online URL for this paper:
<http://eprints.whiterose.ac.uk/92377/>

Version: Accepted Version

Proceedings Paper:

Schiffer, JF, Fridman, E and Ortega, R (2015) Stability of a Class of Delayed Port-Hamiltonian Systems with Application to Droop-Controlled Microgrids. In: IEEE Conference on Decision and Control. 54th Annual Conference on Decision and Control, 15-18 Dec 2015, Osaka, Japan. Institute of Electrical and Electronics Engineers (IEEE) . ISBN 978-1-4799-7884-7

<https://doi.org/10.1109/CDC.2015.7403226>

Reuse

Unless indicated otherwise, fulltext items are protected by copyright with all rights reserved. The copyright exception in section 29 of the Copyright, Designs and Patents Act 1988 allows the making of a single copy solely for the purpose of non-commercial research or private study within the limits of fair dealing. The publisher or other rights-holder may allow further reproduction and re-use of this version - refer to the White Rose Research Online record for this item. Where records identify the publisher as the copyright holder, users can verify any specific terms of use on the publisher's website.

Takedown

If you consider content in White Rose Research Online to be in breach of UK law, please notify us by emailing eprints@whiterose.ac.uk including the URL of the record and the reason for the withdrawal request.



eprints@whiterose.ac.uk
<https://eprints.whiterose.ac.uk/>

Stability of a class of delayed port-Hamiltonian systems with application to droop-controlled microgrids

Johannes Schiffer, Emilia Fridman, Romeo Ortega

Abstract—A class of port-Hamiltonian systems with delayed interconnection matrices is considered. This class of systems is motivated by the problem of stability in droop-controlled microgrids with delays. Delay-dependent stability conditions are derived via the Lyapunov-Krasovskii method. The stability conditions are applied to an exemplary microgrid. The efficiency of the results is illustrated via a simulation example.

I. INTRODUCTION

Time delays are a non-negligible phenomenon in many engineering applications, such as networked control systems, biological systems or chemical processes [1]. In particular, the presence of time delays does often have a significant impact on stability properties of equilibria of a system. Hence, guaranteeing robustness with respect to time delays is of paramount importance in a large variety of applications.

The main motivation for the present work is the analysis of the effect of time delays on the operation of microgrids (μ Gs). The μ G is an emerging concept in the context of electrical networks with large shares of renewable distributed generation (DG) units [2]. μ Gs have been identified as a key component in future power systems [2]. In short, a μ G is a locally controllable subset of a larger electrical grid and is composed of several DG units, storage devices and loads [2]. A key feature of such grids is that they can be operated either in grid-connected or in islanded mode. The latter operation mode increases the reliability of power supply, as it permits to run the μ G completely isolated from the main power system.

In conventional power systems, most generation units are interfaced to the grid via synchronous generators (SGs). In contrast, most renewable DG units are connected to the network via AC inverters. The latter are power electronic devices, which possess significantly different physical properties from SGs [3]. Hence, new control schemes for networks with large shares of inverter-interfaced units are required [3].

A widely-promoted control scheme to operate inverter-interfaced DG units in μ Gs is droop control [4]. This is a decentralized proportional control, the main objectives of which are stability and power sharing. For stability analysis of droop-controlled μ Gs, it is customary to model inverter-interfaced DG units as ideal controllable voltage sources. With this model conditions for stability of droop-controlled μ Gs have been derived, e.g., in [5]–[7].

J. Schiffer is with Technische Universität Berlin, Germany, schiffer@control.tu-berlin.de

E. Fridman is with Tel-Aviv University, Israel emilia@eng.tau.ac.il

R. Ortega is with Laboratoire des Signaux et Systèmes, École Supérieure d'Electricité (SUPELEC), Gif-sur-Yvette 91192, France, ortega@lss.supelec.fr

This work was partially supported by the Israel Science Foundation (grant no. 1128/14).

In a practical setup, the droop control scheme is applied to an inverter by means of digital discrete time control. Digital control usually introduces additional effects such as clock drifts [8] and time delays [9], [10], which may have a deteriorating impact on the system performance. According to [10], the main reasons for the appearance of time delays are 1) sampling of control variables, 2) calculation time of the digital controller and 3) generation of the pulse-width-modulation (PWM) to determine the switching signals for the inverter. This fact has not been considered in the previous work [5]–[7] and in [11] only for the special case of a μ G composed of two inverters. We refer the reader to, e.g., [10] for further details.

With regards to clock drifts, it is shown in [8] that stability of droop-controlled μ Gs is robust with respect to constant unknown clock drifts. Therefore, this phenomenon is neglected in the present paper. Instead, we focus on the impact of time delays on stability of droop-controlled μ Gs. To this end, and following our previous work [6], we represent the μ G as a port-Hamiltonian (pH) system with delays. The main advantage of a pH representation is that the Hamiltonian usually is a natural candidate Lyapunov function.

Stability analysis of pH systems with delays has been subject of previous research [12]–[15]. The main motivation of the aforementioned work is a scenario in which several pH systems are interconnected via feedback paths which exhibit a delay. This setup yields a closed-loop system with skew-symmetric interconnections, which can be split into non-delayed skew-symmetric and delayed skew-symmetric interconnections. However, the model of a droop-controlled μ G with delays derived in this work is not comprised in the class of pH systems studied in [12]–[15], since the delays do not appear skew-symmetrically. In that regard, the class of systems considered in the present work generalizes the class studied in [12]–[15], see Section III for further details. Moreover, compared to [12], [14], [15], we focus on stability in the presence of fast-varying delays, typically arising in the context of digital control [16], [17].

In summary, the main contributions of the present paper are (i) to introduce a model of a droop-controlled μ G, in which the inverters exhibit an input delay, (ii) to represent this μ G model as a pH system with delays, (iii) to provide stability conditions for a class of pH systems with fast-varying delays via the Lyapunov-Krasovskii (LK) method, (iv) to illustrate the utility of the derived conditions on an exemplary μ G.

In addition, we provide an estimate of the region of attraction of a non-delayed μ G as an independent result. To the best of our knowledge, there are no available analytic conditions for estimating the region of attraction of μ Gs and only very few for power systems [18].

Notation. We define the sets $\bar{n} := \{1, 2, \dots, n\}$, $\mathbb{R}_{\geq 0} := \{x \in \mathbb{R} | x \geq 0\}$, $\mathbb{R}_{> 0} := \{x \in \mathbb{R} | x > 0\}$, $\mathbb{R}_{< 0} := \{x \in \mathbb{R} | x < 0\}$, $\mathbb{Z}_{\geq 0} := \{0, 1, 2, \dots\}$ and $\mathbb{S} := [0, 2\pi)$. For a set \mathcal{V} , let $|\mathcal{V}|$ denote its cardinality. For a set of, possibly unordered, positive natural numbers $\mathcal{V} = \{l, k, \dots, n\}$, the short-hand $i \sim \mathcal{V}$ denotes $i = l, k, \dots, n$. Let $x := \text{col}(x_i) \in \mathbb{R}^n$ denote a vector with entries x_i for $i \sim \bar{n}$, $\mathbf{0}_n$ the zero vector, $\mathbf{1}_n$ the vector with all entries equal to one, I_n the $n \times n$ identity matrix, $\mathbf{0}_{n \times n}$ the $n \times n$ matrix with all entries equal to zero and $\text{diag}(a_i), i \sim \bar{n}$, an $n \times n$ diagonal matrix with diagonal entries $a_i \in \mathbb{R}$. Likewise, $A = \text{blkdiag}(A_i)$ denotes a block-diagonal matrix with matrix entries A_i . We employ the notation $\mathcal{I}_{n \times mn} = [I_n, \dots, I_n] \in \mathbb{R}^{n \times mn}$. Let $x \in \mathbb{R}^n$, then $\|x\|$ denotes an arbitrary vector norm. For $A \in \mathbb{R}^{n \times n}$, $A > 0$ means that A is symmetric positive definite. The lower-diagonal elements of a symmetric matrix are denoted by $*$. We denote by $C[-h, 0]$ the space of continuous functions $\phi : [-h, 0] \rightarrow \mathbb{R}^n$. For $x : \mathbb{R}_{\geq 0} \rightarrow \mathbb{R}^n$, we denote $x_t(\sigma_i) = x(t + \sigma_i)$, $\sigma_i \in [-h, 0]$. Also, ∇f denotes the transpose of the gradient of a function $f : \mathbb{R}^n \rightarrow \mathbb{R}$, $\nabla^2 H$ its Hessian matrix, we employ the notation $\nabla \dot{f} = d(\nabla f)/dt$ and if f takes the form $f = f(x(t-h))$, $x \in \mathbb{R}^n$, we use the short-hand $\nabla f_h = \nabla f(x(t-h))$.

II. MOTIVATING APPLICATION: DROOP-CONTROLLED μ GS WITH HETEROGENEOUS DELAYS

A. Network model

We consider a Kron-reduced [19] generic inverter-based μ G in which loads are modeled by constant impedances. The network is composed of $n \geq 1$ inverters and the set of network nodes is denoted by \bar{n} . As done in [5], [6], we assume that the line admittances are purely inductive. Then, two nodes i and k in the network are connected by a nonzero susceptance $B_{ik} \in \mathbb{R}_{< 0}$. The set of neighbors of the i -th node is denoted by $\bar{n}_i = \{k \in \bar{n} | B_{ik} \neq 0\}$. We associate a time-dependent phase angle $\delta_i : \mathbb{R}_{\geq 0} \rightarrow \mathbb{S}$ to each node $i \in \bar{n}$ and use the common short-hand $\delta_{ik} := \delta_i - \delta_k$, $i \in \bar{n}$, $k \in \bar{n}$.

Also, we make the frequent assumption, see, e.g., [5], that the voltage amplitudes $V_i \in \mathbb{R}_{> 0}$ at all nodes $i \in \bar{n}$ are constant. Then, the active power injection $P_i : \mathbb{S}^n \rightarrow \mathbb{R}$ of the i -th inverter is given by [19]¹

$$P_i(\delta_1, \dots, \delta_n) = G_{ii}V_i^2 + \sum_{i \sim \bar{n}_i} a_{ik} \sin(\delta_{ik}), \quad (\text{II.1})$$

where $a_{ik} = |B_{ik}|V_iV_k > 0$ and $G_{ii} \in \mathbb{R}_{\geq 0}$ denotes the shunt conductance at the i -th node.

Finally, we assume that the μ G is connected, i.e., that for all pairs $(i, k) \in \bar{n} \times \bar{n}$, $i \neq k$, there exists an ordered sequence of nodes from i to k such that any pair of consecutive nodes in the sequence is connected by a power line represented by an admittance. This assumption is reasonable for a μ G, unless severe line outages separating the system into several disconnected parts occur.

B. Inverter model with input delay

As outlined in Section I, inverter-based DG units usually exhibit an input delay originating from the fact that they are

¹To simplify notation the time argument of all signals is omitted, whenever clear from the context.

controlled via digital discrete time control [10]. In general, not all inverters in a μ G are identical with respect to their hardware and the implementation of the digital controls. Consequently, the delays are, in general, heterogeneous.

The delay induced by the digital control is typically composed of two main parts: a constant delay $\eta \in \mathbb{R}_{> 0}$ originating from the calculation time of the control signal² and the PWM and an additional delay caused by the sample-and-hold function of control variables [10]. Following [1], [16], we assume that the sampling intervals are bounded, i.e., $t_{\kappa+1} - t_\kappa \leq h_s$, $\kappa \in \mathbb{Z}_{\geq 0}$. Then,

$$t_{\kappa+1} - t_\kappa + \eta \leq h_s + \eta := \bar{h}, \quad (\text{II.2})$$

where \bar{h} denotes the maximum time interval between the time $t_\kappa - \eta$, where the measurement is sampled and the time $t_{\kappa+1}$, where the next control input update arrives.

With these considerations, by following [1], [16] and the usual modeling of inverters, see [8], the inverter at the i -th node with input delay and zero-order-hold update characteristic with sampling instants $t_{i,\kappa}$, can be represented by³

$$\begin{aligned} \dot{\delta}_i(t) &= u_i^\delta(t_{i,\kappa} - \eta_i), \\ \tau_{P_i} \dot{P}_i^m(t) &= -P_i^m(t) + P_i(t), \\ t_{i,\kappa} &\leq t < t_{i,\kappa+1}, \quad \kappa \in \mathbb{Z}_{\geq 0}, \end{aligned} \quad (\text{II.3})$$

where $u_i^\delta : \mathbb{R}_{\geq 0} \rightarrow \mathbb{R}$ is the control input, $\eta_i \in \mathbb{R}_{> 0}$ is a constant delay, P_i is given by (II.1), $P_i^m : \mathbb{R}_{\geq 0} \rightarrow \mathbb{R}$ is the measured active power and $\tau_{P_i} \in \mathbb{R}_{> 0}$ is the time constant of the measurement filter. We assume that the inverters are controlled via the usual frequency droop control given by [4]

$$u_i^\delta(t) = \omega^d - k_{P_i}(P^m(t) - P_i^d). \quad (\text{II.4})$$

C. Closed-loop droop-controlled μ G

As shown in [1], [16], the type of delay appearing in the open-loop system (II.3) results in a fast-varying delay, once the loop is closed. To see this, define $h_i(t) := t - t_{i,\kappa} + \eta_i$, $t_{i,\kappa} \leq t < t_{i,\kappa+1}$. Then, combining (II.3) with (II.4), yields the closed-loop system

$$\begin{aligned} \dot{\delta}_i(t) &= \omega^d - k_{P_i}(P^m(t - h_i(t)) - P_i^d), \\ \tau_{P_i} \dot{P}_i^m(t) &= -P_i^m(t) + P_i(t). \end{aligned} \quad (\text{II.5})$$

Note that (II.2) implies that $\eta_i \leq h_i(t) \leq t_{i,\kappa+1} - t_{i,\kappa} + \eta_i \leq \bar{h}_i$ and $\dot{h}_i(t) = 1$. Via the affine state transformation [6]

$$\begin{bmatrix} \delta_i \\ \omega_i \end{bmatrix} = \begin{bmatrix} 1 & 0 \\ 0 & -k_{P_i} \end{bmatrix} \begin{bmatrix} \delta_i \\ P_i^m \end{bmatrix} + \begin{bmatrix} 0 & 0 \\ 0 & 1 \end{bmatrix} \begin{bmatrix} 0 \\ \omega^d + k_{P_i} P_i^d \end{bmatrix},$$

the system (II.5), (II.4) can be written as

$$\begin{aligned} \dot{\delta}_i(t) &= \omega_i(t - h_i(t)), \\ \tau_{P_i} \dot{\omega}_i(t) &= -\omega_i(t) + \omega^d - k_{P_i}(P_i(t) - P_i^d). \end{aligned} \quad (\text{II.6})$$

It is convenient to introduce the notion of a desired synchronized motion.

²Note that the delay η may also represent the dynamics of the internal control system of the inverter, which is not considered explicitly in the model (II.5). See [20] for a detailed model derivation of the non-delayed version of (II.5).

³An underlying assumption to this model is that whenever the inverter connects an intermittent renewable generation source, e.g., a photovoltaic plant, to the network, it is equipped with some sort of storage (e.g. a battery). Thus, it can increase and decrease its power output within a certain range.

Definition 2.1: A solution $\text{col}(\delta^s, \omega^s \mathbf{1}_n) \in \mathbb{S}^n \times \mathbb{R}^n$ of the system (II.1), (II.6), $i \sim \bar{n}$, is a desired synchronized motion if $\omega^s \in \mathbb{R}_{>0}$ is constant and $\delta^s \in \Theta$, where

$$\Theta := \left\{ \delta \in \mathbb{S}^n \mid |\delta_{ik}| < \frac{\pi}{2}, i \sim \bar{n}, k \sim \bar{n}_i \right\},$$

such that $\delta_{ik}^s = \delta_i^s - \delta_k^s$ are constant, $i \sim \bar{n}$, $k \sim \bar{n}_i$, $\forall t \geq 0$.

Note that along any synchronized motion,

$$\sum_{i \sim \bar{n}} \dot{\omega}_i = 0 \quad \Rightarrow \quad \omega^s = \omega^d + \frac{\sum_{i \sim \bar{n}} (P_i^d - G_{ii} V_i^2)}{\sum_{i \sim \bar{n}} \frac{1}{k_{P_i}}},$$

i.e., for each choice of parameters k_{P_i} and P_i^d , the system (II.1), (II.6), $i \sim \bar{n}$, possesses a unique synchronization frequency, see [5], [6]. We make the following natural power-balance feasibility assumption, see [6].

Assumption 2.2: The system (II.1), (II.6), $i \sim \bar{n}$, possesses a desired synchronized motion.

We denote the vector of phase angles by $\delta = \text{col}(\delta_i) \in \mathbb{S}^n$ and the vector of frequencies $\omega_i = \delta_i$ by $\omega = \text{col}(\omega_i) \in \mathbb{R}^n$. Under Assumption 2.2, we introduce the error states

$$\tilde{\omega}(t) := \omega(t) - \omega^s \mathbf{1}_n \in \mathbb{R}^n, \tilde{\delta}(t) := \delta(0) - \delta^s(0) + \int_0^t \tilde{\omega}(\tau) d\tau \in \mathbb{R}^n.$$

Furthermore, by noting that the power flows (II.1) only depend upon angle differences, we express all angles relative to an arbitrarily chosen reference node, say node n , i.e.,

$$\theta := \mathcal{C} \tilde{\delta}, \quad \mathcal{C} := [I_{(n-1)} \quad -\mathbf{1}_{(n-1)}].$$

For ease of notation, we define the constant $\theta_n := 0$, which is not part of the vector θ . In the reduced angle coordinates, the power flows (II.1) become

$$P_i(\tilde{\delta}(\theta)) = \sum_{k \sim \bar{n}_i} a_{ik} \sin(\theta_{ik} + \delta_{ik}^s). \quad (\text{II.7})$$

By introducing $c_1 := \text{col}(c_{1_i}) \in \mathbb{R}^n$, $c_{1_i} := \omega^d - \omega^s + k_{P_i} P_i^d$, as well as the matrices $K_P = \text{diag}(k_{P_i}) \in \mathbb{R}^{n \times n}$, $T_P = \text{diag}(\tau_{P_i}) \in \mathbb{R}^{n \times n}$, the error dynamics of (II.6), (II.7), $i \sim \bar{n}$, are given in the coordinates $x := \text{col}(\theta, \tilde{\omega}) \in \mathbb{R}^{(n-1)} \times \mathbb{R}^n$ by

$$\begin{aligned} \dot{\theta}(t) &= \mathcal{C} \tilde{\omega}, \\ T_P \dot{\tilde{\omega}}(t) &= -\tilde{\omega}(t) - K_P P(\tilde{\delta}(\theta)) + c_1, \end{aligned} \quad (\text{II.8})$$

where $\tilde{\omega}_h := \text{col}(\tilde{\omega}_i(t - h_i)) \in C[-h, 0]^n$, $h = \max_{i \sim \bar{n}} \bar{h}_i$ and $P(\tilde{\delta}(\theta)) = \text{col}(P_i(\tilde{\delta}(\theta))) \in \mathbb{R}^n$ with $P_i(\tilde{\delta}(\theta))$ given in (II.1). Note that the system (II.8) possesses an equilibrium point $x^s = \mathbf{0}_{2n-1}$, the asymptotic stability of which implies asymptotic convergence of all trajectories of the system (II.6), (II.7), $i \sim \bar{n}$, to the synchronized motion (up to a uniform shift of all angles).

We are interested in the following problem.

Problem 2.3: Consider the system (II.6), (II.7), $i \sim \bar{n}$ with Assumption 2.2. Given \bar{h}_i , $i \sim \bar{n}$, derive conditions, such that the corresponding equilibrium point of (II.8) is (locally) asymptotically stable.

Note that it follows from Proposition 5.9 in [6] that with Assumption 2.2 and for $h_i = 0$, $i \sim \bar{n}$, i.e., the non-delayed version of (II.8), the equilibrium point $x^s = \mathbf{0}_{2n-1}$ is locally asymptotically stable for any choice of T_P , K_P and P^d .

III. A CLASS OF PH SYSTEMS WITH DELAYS

To address Problem 2.3 and by following the analysis in [6], we note that with $x = \text{col}(\theta, \tilde{\omega}) \in \mathbb{R}^{n-1} \times \mathbb{R}^n$ the system

(II.8) can be written as a perturbed pH system with delays

$$\dot{x} = (\mathcal{J} - \mathcal{R}) \nabla H + \sum_{i \sim \bar{n}} \mathcal{T}_i (\nabla H_{h_i} - \nabla H), \quad (\text{III.1})$$

with Hamiltonian $H : \mathbb{R}^{(n-1)} \times \mathbb{R}^n \rightarrow \mathbb{R}$

$$H(x) = \sum_{i=1}^n \left(\frac{\tau_{P_i}}{2k_{P_i}} \tilde{\omega}_i^2 - \frac{1}{2} \sum_{k \sim \bar{n}_i} a_{ik} \cos(\theta_{ik} + \delta_{ik}^s) \right) - \sum_{i=1}^{n-1} \frac{c_{1_i}}{k_{P_i}} \theta_i, \quad (\text{III.2})$$

interconnection matrix

$$\mathcal{J} = \begin{bmatrix} 0_{(n-1) \times (n-1)} & \mathcal{C} K_P T_P^{-1} \\ -(\mathcal{C} K_P T_P^{-1})^\top & 0_{n \times n} \end{bmatrix},$$

damping matrix $\mathcal{R} = \text{diag}(0_{(n-1)}, K_P (T_P^{-2}) \mathbf{1}_n)$ and $\mathcal{T}_i = \mathcal{J} M_i$, where $M_i \in \mathbb{R}^{(2n-1) \times (2n-1)}$, the $(n-1+i, n-1+i)$ -th entry of M_i is one and all its other entries are zero.

Given this fact, it seems natural to analyze (II.8) by exploiting its pH structure (III.1). Hence, for our analysis, we consider a generic nonlinear time-delay system in perturbed Hamiltonian form

$$\dot{x} = (\mathcal{J}(x) - \mathcal{R}(x)) \nabla H + \sum_{i=1}^m (\mathcal{T}_i (\nabla H_{h_i} - \nabla H)), \quad (\text{III.3})$$

with state vector $x : \mathbb{R}_{\geq 0} \rightarrow \mathbb{R}^n$, $m > 0$ delays $h_i : \mathbb{R}_{\geq 0} \rightarrow \mathbb{R}_{>0}$, $h_i(t) \in [0, \bar{h}_i]$, $\bar{h}_i \in \mathbb{R}_{\geq 0}$, $\dot{h}_i(t) = 1$, Hamiltonian $H : \mathbb{R}^n \rightarrow \mathbb{R}$, matrices $\mathcal{J}(x) = -\mathcal{J}(x)^\top \in \mathbb{R}^{n \times n}$, $\mathcal{R}(x) \geq 0 \in \mathbb{R}^{n \times n}$, the entries of which depend smoothly on x , and $\mathcal{T}_i \in \mathbb{R}^{n \times n}$, $i = 1, \dots, m$.

In [12]–[15], stability conditions have been derived for pH systems with time delays of the form

$$\dot{x} = (\mathcal{J}(x) - \mathcal{R}(x)) \nabla H + \sum_{i=1}^m \mathcal{T}_i \nabla H_{h_i}, \quad (\text{III.4})$$

where \mathcal{T}_i are arbitrary interconnection matrices and h_i are time-varying delays. It is easily verified that the system (II.8) cannot be written in the form (III.4). Furthermore, the class of systems (III.4) is a special case of the class (III.3) considered in this paper. To see this, consider two pH systems

$$\begin{aligned} \dot{x}_1 &= (\mathcal{J}_1(x_1) - \mathcal{R}_1) \nabla H_1 + \zeta_1 u_1, & y_1 &= \zeta_1^\top \nabla H_1, \\ \dot{x}_2 &= (\mathcal{J}_2(x_2) - \mathcal{R}_2) \nabla H_2 + \zeta_2 u_2, & y_2 &= \zeta_2^\top \nabla H_2 \end{aligned} \quad (\text{III.5})$$

and feedback interconnections

$$u_2 = y_1(t - h(t)), \quad u_1 = y_2(t - h(t)), \quad (\text{III.6})$$

where $h(t)$ is a transmission delay (uniform, for ease of presentation). Then, the resulting closed-loop system is of the form (III.3), i.e., $\dot{x} = (\mathcal{J}(x) - \mathcal{R}) \nabla H + \mathcal{T}_1 (\nabla H_h - \nabla H)$. In addition, consider a scenario in which the delay appears only in one of the feedback interconnections of (III.6), then the system (III.5), (III.6) also takes the form (III.3).

IV. DELAY-DEPENDENT STABILITY CONDITIONS FOR FAST-VARYING DELAYS

This section is dedicated to the stability analysis of pH systems with bounded fast-varying delays represented by (III.3). The employed approach is based on a strict LK functional. To streamline our main result, we note that

$$\nabla \dot{H} = \nabla^2 H \left((\mathcal{J} - \mathcal{R} - \sum_{i=1}^m \mathcal{T}_i) \nabla H + \sum_{i=1}^m \mathcal{T}_i \nabla H_{h_i} \right) \quad (\text{IV.1})$$

and make the assumptions below.

Assumption 4.1: The system (III.3) possesses an equilibrium point $x^s = \underline{0}_n \in \mathbb{R}^n$.

Assumption 4.2: Consider the system (III.3) with Assumption 4.1 and set $h_i = 0, i \sim \bar{n}$. Then, the equilibrium point x^s of the system (III.3) is (locally) asymptotically stable with Lyapunov function $V_1 = H$.

Our main result is as follows.

Proposition 4.3: Consider the system (III.3) with Assumptions 4.1 and 4.2. Given $\bar{h}_i \geq 0, i = 1, \dots, m$, if there exist $n \times n$ matrices $Y > 0, R_i > 0, S_i > 0$ and $S_{12,i}, i = 1, \dots, m$, such that

$$\begin{bmatrix} \Phi_{11} & \Phi_{12} & \Phi_{13} \\ * & -S - R & R - S_{12}^\top \\ * & * & \Phi_{33} \end{bmatrix} < 0, \quad (\text{IV.2})$$

where

$$\begin{aligned} R &= \text{blkdiag}(R_i), \quad S = \text{blkdiag}(S_i), \quad S_{12} = \text{blkdiag}(S_{12,i}), \\ \mathcal{W} &= \nabla^2 H(\mathcal{J} - \mathcal{R} - \sum_{i=1}^m \mathcal{T}_i), \quad \mathcal{M} = \nabla^2 H \mathcal{L}_{n \times nm}, \\ \mathcal{B} &= [\mathcal{T}_1^\top (R_1 - S_{12,1}) \dots \mathcal{T}_m^\top (R_m - S_{12,m})], \\ \Phi_{11} &= -\mathcal{R} - 0.5 \left(\sum_{i=1}^m \mathcal{T}_i + \sum_{i=1}^m \mathcal{T}_i^\top \right) + \mathcal{W}^\top Y + Y \mathcal{W} \\ &\quad + \sum_{i=1}^m \left(\bar{h}_i^2 (\mathcal{T}_i \mathcal{W})^\top R_i (\mathcal{T}_i \mathcal{W}) + \mathcal{T}_i^\top (S_i - R_i) \mathcal{T}_i \right), \\ \Phi_{12} &= [\mathcal{T}_1^\top S_{12,1} \dots \mathcal{T}_m^\top S_{12,m}], \\ \Phi_{13} &= 0.5 \mathcal{L}_{n \times nm} + \left(Y + \sum_{i=1}^m \bar{h}_i^2 ((\mathcal{T}_i \mathcal{W})^\top R_i \mathcal{T}_i) \right) \mathcal{M} + \mathcal{B}, \\ \Phi_{33} &= \text{blkdiag}(-2R_i + S_{12,i} + S_{12,i}^\top) \\ &\quad + \sum_{i=1}^m \bar{h}_i^2 (\mathcal{T}_i \mathcal{M})^\top R_i (\mathcal{T}_i \mathcal{M}), \end{aligned} \quad (\text{IV.3})$$

and

$$\begin{bmatrix} R & S_{12} \\ * & R \end{bmatrix} \geq 0 \quad (\text{IV.4})$$

are feasible in a neighborhood of x^s , then the equilibrium x^s is (locally) uniformly asymptotically stable for all fast-varying delays $h_i(t) \in [0, \bar{h}_i], i = 1, \dots, m$.

Proof: Inspired by [14], [17], [21], let $h = \max_{i \sim \bar{n}} \bar{h}_i$ and consider the LK functional $V : C[-h, 0]^n \rightarrow \mathbb{R}$,

$$\begin{aligned} V &= V_1 + V_2 + \sum_{i=1}^m (V_{3_i} + V_{4_i}), \quad V_1 = H, \\ V_2 &= \nabla H^\top Y \nabla H, \quad V_{3_i} = \bar{h}_i \int_{-\bar{h}_i}^0 \int_{t+\phi}^t \sigma_i(s) ds d\phi, \quad (\text{IV.5}) \\ V_{4_i} &= \int_{t-\bar{h}_i}^t (\mathcal{T}_i \nabla H(s))^\top S_i (\mathcal{T}_i \nabla H(s)) ds, \end{aligned}$$

where $\sigma_i(s) = (\mathcal{T}_i \nabla \dot{H}(s))^\top R_i (\mathcal{T}_i \nabla \dot{H}(s)), i = 1, \dots, m$. Under the made assumptions H is (locally) positive definite around x^s and $\nabla H|_{x^s} = \underline{0}_n$, which implies that V is an admissible LK functional for the system (III.3) with equilibrium point x^s . Let $\zeta \in \mathbb{R}^{(2m+1)n}$,

$$\zeta = \text{col}(\nabla H, \mathcal{T}_1 \nabla H_{\bar{h}_1}, \dots, \mathcal{T}_m \nabla H_{\bar{h}_m}, \mathcal{T}_1 \nabla H_{h_1}, \dots, \mathcal{T}_m \nabla H_{h_m}).$$

The time-derivative of V_1 is given by

$$\dot{V}_1 = \zeta^\top \begin{bmatrix} -\mathcal{R} - 0.5(\mathcal{T}^\top + \mathcal{T}) & 0_{n \times mn} & 0.5 \mathcal{L}_{n \times mn} \\ * & 0_{mn \times mn} & 0_{mn \times mn} \\ * & * & 0_{mn \times mn} \end{bmatrix} \zeta,$$

where $\mathcal{T} = \sum_{i=1}^m \mathcal{T}_i$. With $\nabla \dot{H}$ given by (IV.1) and \mathcal{W} given in (IV.3), we have that

$$\dot{V}_2 = \zeta^\top \begin{bmatrix} \mathcal{W}^\top Y + Y \mathcal{W} & 0_{n \times mn} & Y \mathcal{M} \\ * & 0_{mn \times mn} & 0_{mn \times mn} \\ * & * & 0_{mn \times mn} \end{bmatrix} \zeta,$$

with \mathcal{M} given in (IV.3). Furthermore,

$$\dot{V}_{3_i} = \bar{h}_i^2 \sigma_i(s) - \bar{h}_i \int_{t-\bar{h}_i}^t \sigma_i(s) ds,$$

where

$$\sigma_i(s) = \zeta^\top \begin{bmatrix} (\mathcal{T}_i \mathcal{W})^\top R_i (\mathcal{T}_i \mathcal{W}) & 0_{n \times nm} & (\mathcal{T}_i \mathcal{W})^\top R_i \mathcal{T}_i \mathcal{M} \\ * & 0_{nm \times nm} & 0_{nm \times nm} \\ * & * & (\mathcal{T}_i \mathcal{M})^\top R_i \mathcal{T}_i \mathcal{M} \end{bmatrix} \zeta,$$

with \mathcal{M} given in (IV.3). By following [17],

$$-\int_{t-\bar{h}_i}^t \sigma_i(s) ds = -\int_{t-\bar{h}_i}^{t-h_i(t)} \sigma_i(s) ds - \int_{t-h_i(t)}^t \sigma_i(s) ds. \quad (\text{IV.6})$$

Suppose that the LMI (IV.4) is feasible. Applying Jensen's inequality together with Lemma 1 in [17], see also [22], to both right hand side terms in (IV.6) yields⁴

$$-\bar{h}_i \int_{t-\bar{h}_i}^t \sigma_i(s) ds \leq - \begin{bmatrix} e_{i1} \\ e_{i2} \end{bmatrix}^\top \begin{bmatrix} R_i & S_{12,i} \\ * & R_i \end{bmatrix} \begin{bmatrix} e_{i1} \\ e_{i2} \end{bmatrix}, \quad i = 1, \dots, m,$$

with $e_{i1} = \mathcal{T}_i (\nabla H - \nabla H_{h_i})$ and $e_{i2} = \mathcal{T}_i (\nabla H_{h_i} - \nabla H_{\bar{h}_i})$. Hence,

$$\begin{aligned} \sum_{i=1}^m \left(-\bar{h}_i \int_{t-\bar{h}_i}^t \sigma_i(s) ds \right) &\leq \\ \zeta^\top \begin{bmatrix} -\sum_{i=1}^m (\mathcal{T}_i^\top R_i \mathcal{T}_i) & \Phi_{12} & \mathcal{B} \\ * & -R & R - S_{12}^\top \\ * & * & -2R + S_{12} + S_{12}^\top \end{bmatrix} \zeta, \end{aligned}$$

where $R, S, S_{12}, \mathcal{B}$ and Φ_{12} are defined in (IV.3). In addition,

$$\dot{V}_{4_i} = (\mathcal{T}_i \nabla H)^\top S_i (\mathcal{T}_i \nabla H) - (\mathcal{T}_i \nabla H_{\bar{h}_i})^\top S_i (\mathcal{T}_i \nabla H_{\bar{h}_i}).$$

Consequently, if

$$\dot{V} \leq \zeta^\top \begin{bmatrix} \Phi_{11} & \Phi_{12} & \Phi_{13} \\ * & -S - R & R - S_{12}^\top \\ * & * & \Phi_{33} \end{bmatrix} \zeta,$$

where $\Phi_{11}, \Phi_{12}, \Phi_{13}$ and Φ_{22} are defined in (IV.3). Clearly, if (IV.2) is feasible, then $\dot{V} \leq -\varepsilon \|x(t)\|^2$ for some $\varepsilon > 0$. The proof is completed by invoking the LK theorem, see, e.g., Theorem 1 in [17] and arguments from [24] for systems with piecewise-continuous delays. ■

Remark 4.4: The conditions given in Proposition 4.3 are state-dependent. We note that, in many cases, the conditions can be conveniently implemented numerically via a polytopic approach [1], [15]. This is also the procedure taken in Section V of the present paper to investigate stability of an equilibrium of the system (II.8).

⁴Note that instead of Jensen's inequality, also Wirtinger's inequality [15] could be employed to upper bound the terms $-\bar{h}_i \int_{t-\bar{h}_i}^t (\mathcal{T}_i \nabla \dot{H}(s))^\top R_i (\mathcal{T}_i \nabla \dot{H}(s)) ds, i = 1, \dots, m$. In particular, this could prove useful when considering a more complicated augmented LK functional, see [23].

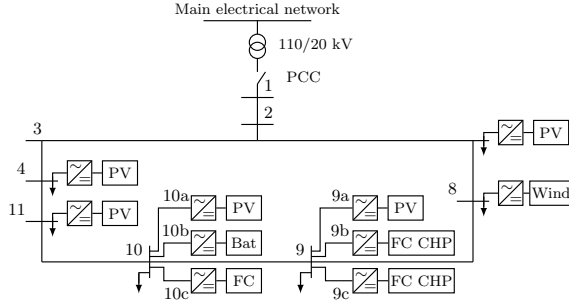


Fig. 1. Benchmark model adapted from [25] with 6 main buses and inverter-interfaced units of type: PV–Photovoltaic, FC–fuel cell, Bat–battery, FC CHP. PCC denotes the point of common coupling to the main grid. The sign \downarrow denotes loads.

V. NUMERICAL EXAMPLE

Proposition 4.3 is illustrated via a numerical example based on the inner ring of the islanded Subnetwork 1 of the CIGRE benchmark MV distribution network [25]. The network consists of eight main buses and is shown in Fig. 1. We assume that the generation sources at buses 9b, 9c, 10b and 10c are operated with droop control, while the remaining sources are operated in PQ-mode [20]. See [25] or [6] for a detailed discussion of the employed benchmark model. Furthermore, we associate to each inverter a power rating $S^N = [0.517, 0.353, 0.333, 0.023]$ pu, where pu denotes per unit values with respect to the base power $S_{\text{base}} = 3$ MVA. Following Lemma 6.2 in [6], we select $P_i^d = 0.6S_i^N$ pu and $k_{P_i} = 0.2/S_i^N$ Hz/pu, $i \sim \bar{n}$. The low pass filter time constants are set to $\tau_P = [0.1, 0.6, 0.8, 0.2]$ s.

A. Estimate of region of attraction of non-delayed system

As the conditions given in Proposition 4.3 are state-dependent, to perform a numerical analysis, it is useful to obtain an estimate of a meaningful region of the state-space in which the conditions of Proposition 4.3 shall be satisfied. Here, we address this issue by deriving an estimate of the region of attraction of the non-delayed version of system (III.1). An extension to the delayed case may be of potential interest and we plan to address this aspect in the future.

Besides, estimating the region of attraction in μ Gs and power systems is an interesting and challenging problem on its own [18]. In that regard, we remark that the result below is an independent result for the non-delayed model of (III.1).

Lemma 5.1: Consider the system (III.1) with Assumption 2.2 and $\bar{h}_i = 0$, $i \sim \bar{n}$. Fix a small positive number ϑ , such that $|\theta_{ik} + \delta_{ik}^s| < \frac{\pi}{2} - \vartheta$, $i \sim \bar{n}$, $k \sim \bar{n}_i$ and an arbitrarily large positive number $\beta \gg \vartheta$. Estimates of the domain of attraction of the asymptotically stable equilibrium point $x^s = \underline{0}_{2n-1}$ are the sublevel sets

$$\Omega_c = \{x = \text{col}(\theta, \tilde{\omega}) \in \mathbb{R}^{(2n-1)} \mid H(x) \leq c\},$$

that are contained in

$$\begin{aligned} \mathcal{D} &= \{x \in \mathbb{R}^{(2n-1)} \mid \|x\| \leq \beta, \\ &|\theta_{ik} + \delta_{ik}^s| \leq \frac{\pi}{2} - \vartheta, i \sim \bar{n}, k \sim \bar{n}_i\}. \end{aligned}$$

Proof: Following [26], the claim is established by exploiting properties of sublevel sets of strongly convex closed functions together with the fact that from (III.1) it

follows that

$$\dot{H} = -\nabla H^\top R \nabla H \leq 0 \quad \forall x \in \mathbb{R}^{(2n-1)}. \quad (\text{V.1})$$

We start by noting that the continuity of H defined in (III.2) together with the fact that \mathcal{D} is a closed set implies that H is a closed function on \mathcal{D} , cf. A.3.3 of [27]. Hence, the sublevel sets of H on \mathcal{D} are closed, cf. A.3.3 of [27].

Next, we establish boundedness of the sublevel sets of H contained in \mathcal{D} . To this end, we recall the fact that if H in (III.2) is a strongly convex closed function on some set $\mathcal{S}_\epsilon \subset \mathbb{R}^{(2n-1)}$, then the sublevel sets of H contained in \mathcal{S}_ϵ are bounded, cf. Chapter 9 of [27]⁵. Strong convexity of H on some set $\mathcal{S}_\epsilon \subset \mathbb{R}^{(2n-1)}$ is equivalent to $\nabla^2 H \geq \epsilon I_{(2n-1)}$ for some positive real ϵ and all $x \in \mathcal{S}_\epsilon$, cf. Chapter 9, [27]. For H given in (III.2), we have that

$$\nabla^2 H = \begin{bmatrix} \mathcal{L}(\theta) & \underline{0}_{(n-1) \times n} \\ * & \text{diag}(\tau_{P_i}/k_{P_i}) \end{bmatrix},$$

where $\mathcal{L} : \mathbb{R}^{(n-1)} \rightarrow \mathbb{R}^{(n-1) \times (n-1)}$ with $l_{ii} = \sum_{k \sim \bar{n}} a_{ik} \cos(\theta_{ik} + \delta_{ik}^s)$, $l_{ip} = -a_{ip} \cos(\theta_{ip} + \delta_{ip}^s)$, $i \sim \bar{n} \setminus \{n\}$, $p \sim \bar{n} \setminus \{n\}$. The image of \mathcal{L} on the compact domain $\mathcal{D}_\theta := \{\theta \in \mathbb{R}^{n-1} \mid |\theta_{ik} + \delta_{ik}^s| \leq \frac{\pi}{2} - \vartheta, i \sim \bar{n}, k \sim \bar{n}_i\}$ (recall from Section II-C that $\theta_n = 0$ is a constant) is given by the matrix polytope $\mathcal{L}^P = \{\mathcal{L} = \sum_{i=1}^q \alpha_i \mathcal{L}_i \mid \alpha_i \geq 0, \sum_{i=1}^q \alpha_i = 1\}$, where $m \leq n(n-1)/2$ is the number of angle differences and $q = 2^m$ the number of vertices \mathcal{L}_i of the polytope. Denote the $n-1$ eigenvalues of a matrix $\mathcal{L} \in \mathcal{L}^P$ by λ_k , $k = 1, \dots, n-1$. It follows from Lemma 5.8 in [6] that $\lambda_k > 0$, $k = 1, \dots, n-1$, for any $\mathcal{L} \in \mathcal{L}^P$. Following [28], define the eigenvalue set of the matrix polytope \mathcal{L}^P by $\Lambda(\mathcal{L}^P) := \{\lambda_k(\mathcal{L}), k = 1, \dots, n-1, \mathcal{L} \in \mathcal{L}^P\}$. Denote the convex hull of all eigenvalues of all vertex matrices \mathcal{L}_i , $i = 1, \dots, q$, by $\text{conv}\{\lambda_k(\mathcal{L}_i), k = 1, \dots, n-1, i = 1, \dots, q\}$. Note that any \mathcal{L}_i , $i = 1, \dots, q$, is symmetric and, hence, normal. Then, by Theorem 1 in [28], $\Lambda(\mathcal{L}^P) \subset \text{conv}\{\lambda_k(\mathcal{L}_i), k = 1, \dots, n-1, i = 1, \dots, q\}$. Let $\gamma := \min_{\lambda_k} \text{conv}\{\lambda_k(\mathcal{L}_i), k = 1, \dots, n-1, i = 1, \dots, q\} > 0$. Clearly, there also exists a constant $0 < \epsilon < \min\left(\gamma, \min_{i \sim \bar{n}} \left(\frac{\tau_{P_i}}{k_{P_i}}\right)\right)$, such that $\nabla^2 H \geq \epsilon I_{(2n-1)}$, $\forall \text{col}(\theta, \tilde{\omega}) \in \mathcal{D}$. This proves that H is strongly convex on \mathcal{D} , which implies that the sublevel sets $\Omega_c = \{x \in \mathbb{R}^{(2n-1)} \mid H(x) \leq c\}$ contained in \mathcal{D} are bounded.

Summarizing, we have shown that the sublevel sets of H contained in \mathcal{D} are closed and bounded, hence compact. The proof is completed by noting that (V.1) implies that all sublevel sets of H contained in \mathcal{D} are positively invariant. ■

B. Stability analysis

We set $m = 4$ and $\bar{h}_i = \bar{h} \in \mathbb{R}_{>0}$, $i \sim \bar{n}$, in the numerical analysis, i.e., we assume that all droop-controlled units exhibit a delay with the same upper bound. Furthermore, we recall the set \mathcal{D} defined in Lemma 5.1 and note that for the considered scenario a feasible choice is $\vartheta = 10^{-8}$. The numerical implementation of the conditions (IV.2), (IV.4) is done using Yalmip [29]. To this end, we note that in the present case the variables θ_i only appear as arguments of the cos-function in condition (IV.2). Therefore, it is fairly

⁵Note that strong convexity is a sufficient, not a necessary condition for boundedness of sublevel sets [26], [27].

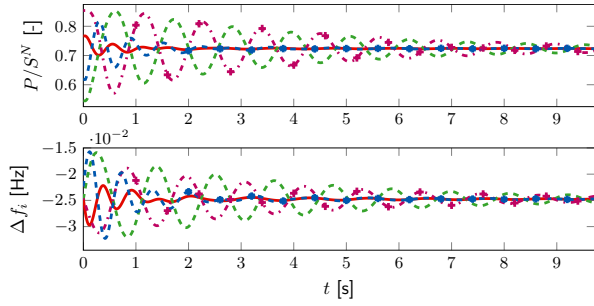


Fig. 2. Simulation example of a droop-controlled μG with fast-varying delays with $\bar{h}_i = 0.04$, $i \sim \bar{n}$. Trajectories of the power outputs relative to source rating P_i/S_i^N , and the inverter frequencies $f_i = 2\pi\omega_i$ in Hz of the controllable sources in the μG . The lines correspond to the following sources: FC CHP 9b, $i = 1$ ‘-’, FC CHP 9c, $i = 2$ ‘-’, battery 10b, $i = 3$ ‘+’ and FC 10c, $i = 4$ ‘*’.

straight-forward to adopt a polytopic approach, i.e., to represent the set $\{\nabla^2 H(x) \mid x \in \mathcal{D}\}$ as $\nabla H^2 = \sum_{i=1}^q \alpha_i \nabla^2 H^i$, $0 \leq \alpha_i \leq 1$, $\sum_{i=1}^q \alpha_i = 1$, where $\nabla^2 H^i$ denote the vertices of the polytope containing all instances that $\nabla^2 H$ can take on the set \mathcal{D} , see also the proof of Lemma 5.1. We remark that the region of attraction of the delayed system may, in general, not be identical to \mathcal{D} , yet the feasibility of the conditions of Proposition 4.3 for all vertices $\nabla^2 H^i$ together with the positive definiteness of the LK functional (IV.5) ensures the existence of a compact positively invariant set for initial conditions x_0 close enough to x^s and, thus, local asymptotic stability of x^s . For the considered network, the number of nodes in the Kron-reduced network is 4. Hence, we have $n(n-1)/2 = 6$ angle differences and can describe the set $\{\nabla^2 H(x) \mid x \in \mathcal{D}\}$ with $q = 2^6$ vertices. For the chosen set of parameters, the maximal admissible delay is $\bar{h} = 0.04$.

C. Simulation example

Proposition 4.3 is illustrated via a simulation example. We note that the largest R/X ratio in the Kron-reduced network corresponding to that in Fig. 1 is 0.30. For HV transmission lines it is typically 0.31, see [6]. Thus, the assumption of dominantly inductive admittances is satisfied and the resistive part of the line admittances is neglected in the simulations. The results displayed in Fig. 2 show that the trajectories of the system (II.8) with $\bar{h}_i = 0.04$, $i \sim \bar{n}$, converge to a synchronized motion if the sufficient conditions (IV.2), (IV.4) are satisfied. Here, we have assumed constant sampling intervals $h_{i,s} = 2 \cdot 10^{-4}$, see (II.2). With $\bar{h}_i = 0.04$, the maximum admissible delay in simulation is $1.4\bar{h}_i$. This indicates that the derived sufficient conditions are very effective for the system under investigation. We note that the conditions could be further improved by employing more complex LK functionals, e.g., by using ideas from [16], [23].

VI. CONCLUSIONS

Motivated by the problem of stability in droop-controlled inverter-based μG s with delays, we have provided sufficient delay-dependent conditions for stability of a class of pH systems. The conditions are derived via an LK functional and have proven to be effective in a practical example of a μG . Future work will extend the analysis to μG s with inverter- and SG-interfaced DG units, as well as to more detailed inverter and network models. Also, we seek to provide an estimate of the region of attraction of μG s with delays.

REFERENCES

- [1] E. Fridman, *Introduction to time-delay systems: analysis and control*. Birkhäuser, 2014.
- [2] N. Hatzigiorgiou, H. Asano, R. Irvani, and C. Marnay, “Microgrids,” *IEEE Power and Energy Magazine*, vol. 5, no. 4, pp. 78–94, 2007.
- [3] T. Green and M. Prodanovic, “Control of inverter-based micro-grids,” *Electric Pow. Sys. Research*, vol. Vol. 77, no. 9, pp. 1204–1213, 2007.
- [4] J. Guerrero, P. Loh, M. Chandorkar, and T. Lee, “Advanced control architectures for intelligent microgrids – part I: Decentralized and hierarchical control,” *IEEE Transactions on Industrial Electronics*, vol. 60, no. 4, pp. 1254–1262, 2013.
- [5] J. W. Simpson-Porco, F. Dörfler, and F. Bullo, “Synchronization and power sharing for droop-controlled inverters in islanded microgrids,” *Automatica*, vol. 49, no. 9, pp. 2603 – 2611, 2013.
- [6] J. Schiffer, R. Ortega, A. Astolfi, J. Raisch, and T. Sezi, “Conditions for stability of droop-controlled inverter-based microgrids,” *Automatica*, vol. 50, no. 10, pp. 2457–2469, 2014.
- [7] U. Münz and M. Metzger, “Voltage and angle stability reserve of power systems with renewable generation,” in *19th IFAC World Congress*, Cape Town, South Africa, 2014, pp. 9075–9080.
- [8] J. Schiffer, R. Ortega, C. Hans, and J. Raisch, “Droop-controlled inverter-based microgrids are robust to clock drifts,” in *ACC*, Chicago, IL, USA, 2015, pp. 2341–2346.
- [9] D. Maksimovic and R. Zane, “Small-signal discrete-time modeling of digitally controlled PWM converters,” *IEEE Transactions on Power Electronics*, vol. 22, no. 6, pp. 2552–2556, 2007.
- [10] T. Nussbaumer, M. L. Heldwein, G. Gong, S. D. Round, and J. W. Kolar, “Comparison of prediction techniques to compensate time delays caused by digital control of a three-phase buck-type PWM rectifier system,” *IEEE Transactions on Industrial Electronics*, vol. 55, no. 2, pp. 791–799, 2008.
- [11] D. Efimov, R. Ortega, and J. Schiffer, “ISS of multistable systems with delays: application to droop-controlled inverter-based microgrids,” in *ACC*, Chicago, IL, USA, 2015, pp. 4664–4669.
- [12] R. Pasumarthy and C.-Y. Kao, “On stability of time delay Hamiltonian systems,” in *ACC*, 2009, pp. 4909–4914.
- [13] R. Yang and Y. Wang, “Stability analysis for a class of nonlinear time-delay systems via hamiltonian functional method,” in *8th World Congress on Intel. Control and Autom.* IEEE, 2010, pp. 2874–2879.
- [14] C.-Y. Kao and R. Pasumarthy, “Stability analysis of interconnected Hamiltonian systems under time delays,” *IET control theory & applications*, vol. 6, no. 4, pp. 570–577, 2012.
- [15] S. Aoues, W. Lombardi, D. Eberard, and A. Seuret, “Robust stability for delayed port-hamiltonian systems using improved wirtinger-based inequality,” in *Conference on Decision and Control*, 2014.
- [16] K. Liu and E. Fridman, “Wirtinger’s inequality and Lyapunov-based sampled-data stabilization,” *Autom.*, vol. 48, no. 1, pp. 102–108, 2012.
- [17] E. Fridman, “Tutorial on Lyapunov-based methods for time-delay systems,” *Europ. Jour. of Control*, vol. 20, no. 6, pp. 271–283, 2014.
- [18] U. Münz and D. Romeres, “Region of attraction of power systems,” in *Estim. and Ctrl. of Networked Syst.*, vol. 4, no. 1, 2013, pp. 49–54.
- [19] P. Kundur, *Power system stability and control*. McGraw-Hill, 1994.
- [20] J. Schiffer, D. Zonetti, R. Ortega, A. Stankovic, T. Sezi, and J. Raisch, “Modeling of microgrids—from fundamental physics to phasors and voltage sources,” *arXiv preprint arXiv:1505.00136*, 2015.
- [21] E. Fridman, M. Dambrine, and N. Yeganefar, “On input-to-state stability of systems with time-delay: A matrix inequalities approach,” *Automatica*, vol. 44, no. 9, pp. 2364–2369, 2008.
- [22] P. Park, J. W. Ko, and C. Jeong, “Reciprocally convex approach to stability of systems with time-varying delays,” *Automatica*, vol. 47, no. 1, pp. 235–238, 2011.
- [23] A. Seuret and F. Gouaisbaut, “Wirtinger-based integral inequality: application to time-delay systems,” *Automatica*, vol. 49, no. 9, pp. 2860–2866, 2013.
- [24] E. Fridman, A. Seuret, and J.-P. Richard, “Robust sampled-data stabilization of linear systems: an input delay approach,” *Automatica*, vol. 40, no. 8, pp. 1441–1446, 2004.
- [25] K. Rudion, A. Orths, Z. Styczynski, and K. Strunz, “Design of benchmark of medium voltage distribution network for investigation of DG integration,” in *IEEE PESGM*, 2006.
- [26] M. Galaz, R. Ortega, A. S. Bazanella, and A. M. Stankovic, “An energy-shaping approach to the design of excitation control of synchronous generators,” *Automatica*, vol. 39, no. 1, pp. 111–119, 2003.
- [27] S. Boyd and L. Vandenberghe, *Convex optimization*. Cambridge university press, 2009.
- [28] Q.-G. Wang, “Necessary and sufficient conditions for stability of a matrix polytope with normal vertex matrices,” *Automatica*, vol. 27, no. 5, pp. 887–888, 1991.
- [29] J. Löfberg, “YALMIP : a toolbox for modeling and optimization in MATLAB,” in *IEEE International Symposium on Computer Aided Control Systems Design*, sept. 2004, pp. 284 –289.